Volume 205, number 2 FEBS 3981 September 1986

Electropore diameters, lifetimes, numbers, and locations in individual erythrocyte ghosts

Arthur E. Sowers° and Michael R. Lieber*+

Biomedical Research and Development, American Red Cross Laboratories, 9312 Old Georgetown Road, Bethesda, MD 20814 and +*Laboratory of Pathology, National Cancer Institute, Bethesda, MD 20205, USA*

Received 14 July 1986

Low light level video microscopy was used to study the diameter, lifetime, number, and location characteristics of electric field-induced pores (electropores) in erythrocyte ghosts. The diameter of electropores was probed by following the efflux of soluble fluorescent-tagged molecules out of the resealed ghost cytoplasmic compartments. After reaching a peak radius of at least 8.4 nm the electropores resealed within 200 ms to a radius of about 0.5 nm and stayed at that radius thereafter. Video sequences clearly show that pores are induced preferentially in the cathodal hemisphere. Pores induced in the hemisphere facing the positive electrode were either (i) never greater than 0.5 nm in radius, (ii) much smaller in number if they were greater than 0.5 nm in radius, or (iii) shorter lived. Calculations indicated that an upper limit of 700 electropores were induced per membrane.

Electroporation *Electropore* *Pore* *Electrofusion* *Fusion* *Erythrocyte ghost*

1. INTRODUCTION

Membrane permeability can be transiently increased by inducing a higher than normal membrane potential by an appropriate electric field pulse (reviews [1–3]). Such increased permeability is widely attributed to pores (electropores). The induction of electropores has found applications in many diverse experiments that require a non-chemical method of permeabilizing membranes. Moreover, the mechanism of the induction of electropores may have fundamental implications for membrane structure and properties. For example, electropores have been proposed to be involved as an intermediate structure in the mechanism of membrane electrofusion [4–7]. In a previous analysis electropores in erythrocyte ghosts were assumed to be similar to electropores in intact erythrocytes [8]. This assumption permitted us to conclude that electropores were unlikely to be involved in the electrofusion mechanism.

Some studies have measured the effective diameters and have estimated the numbers of these electropores by (i) indirect calculations based on the transient increase in electrical conductivity which can be measured after the pulse [9,10], or (ii) monitoring the movement of ionic species or molecules with known radii after the pulse [8–15].

We report here for the first time the

Contribution no.705 from the American Red Cross Laboratories

* Present address: Laboratory of Molecular Biology, NIADDK, NIH, Bethesda, MD 20205, USA
° Address after December 1986: Holland Laboratory for the Biomedical Sciences, 15601 Crabbs Branch Way, Rockville, MD 20855, USA

Abbreviations: B&W, black and white; *D*, diffusion coefficient; *E*, electric field strength; FITC, fluorescein isothiocyanate; FB, fluoresceinated bovine serum albumin; FD, fluoresceinated dextran; FM, fluoresceinated myoglobin; LY, Lucifer Yellow CH; RP, R-phycoerythrin

Published by Elsevier Science Publishers B.V. (Biomedical Division)
00145793/86/$3.50

simultaneous determination of four electropore characteristics in single human erythrocyte ghost membranes. They include the direct measurement of (i) the electropore lifetime, and (ii) the electropore location on the membrane, and a measure (iii) of the lower limit for the effective radius of the electropore, and (iv) a calculated upper limit for electropore numbers. The experimental results of this study support the overall validity of the analysis that electropores are not likely to be involved in the electrofusion mechanism [8].

2. MATERIALS AND METHODS

Isolation of human erythrocyte ghosts and labeling of the ghost cytoplasmic compartments with fluorescent soluble probes (see below), details of the observation chamber, the electrical circuit of the pulse generator, and the microscope optical system were as described [16]. All pulses used here generated a field strength of 700 V/mm at the point of observation in the chamber and had a decay half-time of either 0.6 or 1.2 ms (referred to hereafter as 0.6 or 1.2 ms pulses). The pulse-induced temperature increase was previously shown to be insignificant [8]. All experiments were conducted in 20 mM sodium phosphate buffer (pH 8.5) at 22–24°C. The ultraviolet excitation beam was attenuated with neutral density filters to the point where probe bleaching over the period of the experiment was not perceptible compared to previously unilluminated probe material. Mixtures of 10 μm diameter fluorescent cytometer calibration spheres (Epics, Hialeah, FL) and labeled ghosts were transferred to the observation chamber. Labeled ghost membranes and calibration spheres were immobilized onto the glass surfaces in the chamber with polylysine. The concentration of ghosts was adjusted so that only one or two ghosts were present in a field of view for the efflux measurements. The images of the fluorescent membranes and reference spheres were converted to a standard video signal with a Zeiss (Thornwood, New York) three-stage low light level Venus Camera. Video recordings always included at least one calibration sphere and one ghost. Date and time alphanumerics were generated by a VTG-22 video timer (Fora, West Newton, MA) and then added to the video signal which was then recorded on video tape (since the timer clock was not synchronized with the camera video signal the error between recorded time and real time on any video frame could differ by as much as 0.033 s).

A first approximation of total pore area was obtained as follows. Single frame images were selected from recorded sequences and macrophotographed onto 35 mm B&W film directly from the TV monitor screen. The negative images on the 35 mm film were printed onto 4 × 5 B&W sheet film as positive images and scanned in a one-dimensional gel scanner (set in the optical density mode) along a line which was perpendicular to the background video raster lines and intersected the center of the fluorescent sphere. The overall transfer of intensity data from microscope to densitometer scan curves was found to be within ± 5% as long as the membrane and calibration sphere under study stayed in the same position during the measurements (electropore induction in membranes in suspensions was found to be not significantly different from electropore induction in immobilized membranes). The amount of soluble fluorescent label in each ghost membrane was estimated by normalizing the integrated area under each optical density scan of a ghost image to the area under the scan of the calibration sphere in the same video frame. Total loss of label during a given time interval was obtained by subtracting total fluorescence of a later image from that of an earlier image.

The efflux time courses were analyzed using an integrated form of Fick's first law for two compartment diffusion as described in [17] and outlined here.

$$\ln\left(\frac{(C_{eq} - C_t)}{(C_{eq} - C_0)}\right) = \frac{-DA(1/V_m + 1/V_g)t}{\Delta x} \qquad (1)$$

where C_0, C_{eq}, C_t are the concentrations of the marker molecule inside the cells (mol/cm^3) at zero time (0), at equilibrium (eq) and at intermediate intervals (t, s), respectively. V is the volume of solvent (cm^3/ghost) in the extracorpuscular medium (m) and in the ghost (g). The ghost volume was taken to be 150 μm^3 because the ghosts were at their maximum spherocytic volume under the conditions studied here. Since $V_m >> V_g$, the term $1/V_m$ vanishes. D is the aqueous diffusion coefficient of the solute at 25°C which is 9.4 × 10^{-7} cm^2/s for dextran [18]. Δx is the membrane

thickness, taken here to be 6 nm [17]. A is the average area per ghost available for diffusion from inside to outside the ghosts through holes in the membrane. A' differs from the true hole area, A, because of sieving [18]. Whereas $A = n\pi r^2$, $A' = n\pi(r - a)^2$. The number of holes per ghost is n; r and a are the radii of the holes and marker molecules, respectively.

Assumptions of this method of analysis are (i) marker movement only due to aqueous diffusion and from inside to outside the ghosts, (ii) all n holes in any given ghost are the same radius, and (iii) the membrane holes are cylindrical in configuration.

Two experiments were conducted on labeled membranes: (i) the effect of a single 1.2 ms pulse, and (ii) the effect of four 0.6 ms pulses.

To probe the diameter of the electropores, the following soluble fluorescent molecules were utilized: 6-deoxy-*N*-(7-nitrobenz-2-oxa-1,3-diazol-4-yl)aminoglucose (NBD-G) [19], LY [20], several FDs (average M_r 10000, 70000, or 156000), FM, FB, and RP. These molecules have estimated unhydrated and unconjugated equivalent sphere radii of: 0.45, 0.75 (from C–C bond lengths), 2.3, 5.8, 8.4 (from chromatography [18]), 1.8, 2.8, and 4.3 (from 0.00151 nm^3/Da [21]), respectively. NBD-G was purchased from Molecular Probes (Junction City, OR). All other reagents were purchased from Sigma. The conjugation of FITC to bovine serum albumin and myoglobin was performed as in [22]. A freeze-thaw cycle caused all probes to be released to the medium from loaded ghosts.

3. RESULTS

Regardless of the pulse characteristics, efflux occurred for all fluorescent labels except FB, FM and RP (with buffer pH = 8.5 during ghost resealing). However, efflux of FM occurred if the ghosts were resealed with the buffer pH adjusted to 6.0 (pulse-induced efflux of FB and RP with the buffer adjusted below their isoelectric points was not attempted).

Regardless of whether 0.6 of 1.2 ms pulses were used, each pulse always induced only some of the fluorescence to leave the ghost. Additional pulses eventually caused membranes to lose all visible fluorescence. This showed that (i) after induction the electropores were self-resealing (i.e. reversible at least to a radius equal to or smaller than the probe molecule), and (ii) the labels did not bind to the membranes. If labeled ghosts were added to the chamber in a suspension such that about 100 ghosts could be counted as the focus was adjusted through the depth of the chamber, then the pulse-induced step loss of fluorescence from the labeled compartments was always accompanied by a visible step increase in the background fluorescence. This indicated that any diminution in fluorescence of the marker due to a pulse-induced electrochemical change was insignificant.

Video sequences showed that a distinct cloud of fluorescence appeared outside the hemisphere facing the negative electrode of ghosts loaded with FD (10 kDa) after a single 1.2 ms pulse (fig.1). The cloud began to develop about 20–50 ms after the pulse and was visible until about 200 ms after the pulse. The same results were obtained when LY was used as the soluble fluorescent label (not shown).

Areas under each curve from densitometric scans of selected frames of the sequence in fig.1 are shown in fig.2. The trace shows a loss of 65% of the labeled molecules in the 200 ms interval that followed the single pulse. Loss over the next 1.3 s was 0.05 or less of the original prepulse fluorescence. A single 0.6 or 1.2 ms pulse would induce ghosts loaded with NBD-G to lose continuously and slowly all fluorescence within 1–2 min.

Fig.1 images were analyzed and the data were plotted as a function of time (fig.2) and then replotted according to eqn 1 as $\ln[(C_{eq} - C_t)/(C_{eq} - C_0)]$ as a function of time, t (fig.2, inset). The slope of this plot is -8.7. Solving eqn 1 for the apparent area available for diffusion, A, we have:

$$A' = \frac{\Delta x(\text{slope})(V_g)}{D}$$

$$= 8.4 \times 10^{-10}\ \text{cm}^2 \text{ per ghost}$$

During the existence of the cloud (the total pore area expressed as a fraction of total surface area would be 0.084 μm^2 divided by 140 μm^2 = 0.0006 and, as discussed [8], is still far lower than needed to account for observed fusion yields.

Given that the largest dextran (156 kDa) was

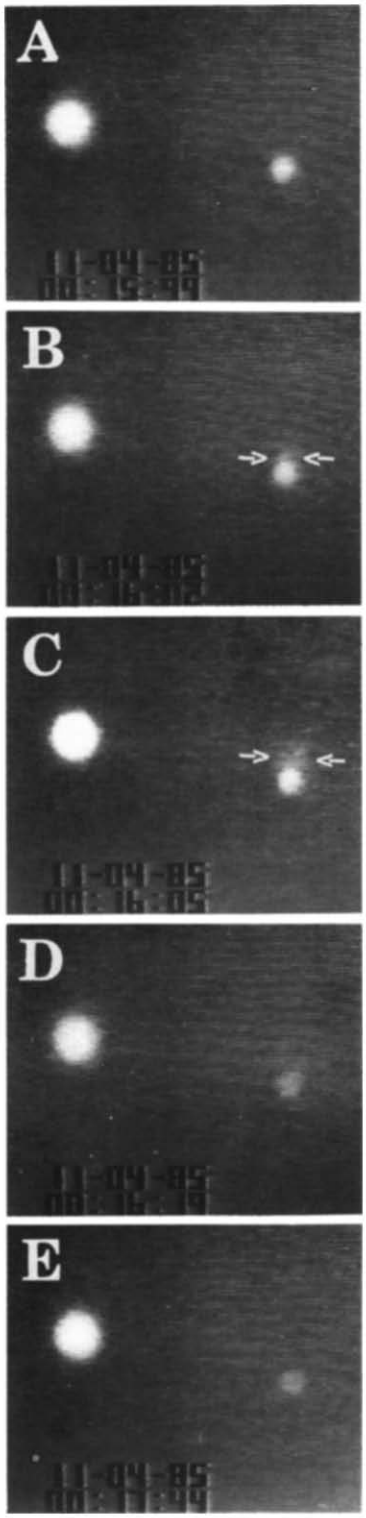

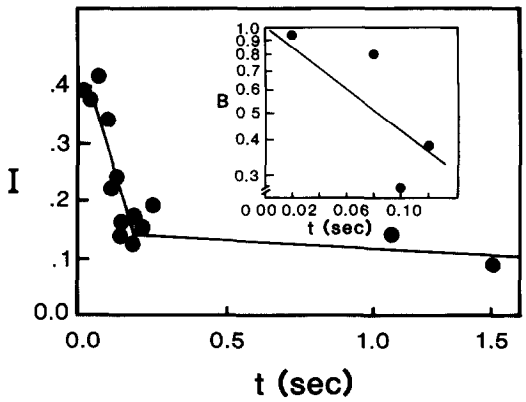

Fig.2. Total integrated fluorescence (arbitrary scale), I, from a single fluorescent labeled ghost (data from frame sequence as shown in fig.1) cytoplasmic compartment as a function of time. Pulse applied at 0.02 s (arrow). Inset: semilog plot of $B = ([C_{eq} - C_t]/[C_{eq} - C_0]) = ([0.16 - C_t]/[0.16 - 0.40])$ as a function of time. Note that not all points are plotted (see text).

able to escape, $r > 8.4$ nm, then

$$n \leqslant A'/\pi(80 \times 10^{-8}\ \text{cm} - 23 \times 10^{-8}\ \text{cm})^2$$

$$\leqslant 702$$

An observable cloud of fluorescence was never seen outside of the FD (10 kDa) loaded ghosts when 0.6 ms pulses were used (not shown). However, incremental decreases in cytoplasmic fluorescence occurred simultaneously with the application of each of these pulses but the magnitude was much smaller. Indeed, densitometric scans showed that the fractional loss per 0.6 ms pulse was smaller (average: 0.15) than per 1.2 ms pulse (average: 0.65). Variability in the fraction of initial

Fig.1. Selected individual video frames showing effect of a single 1.2 ms pulse (electric field strength 700 V/mm) on retention of FITC-dextran (10 kDa) in the cytoplasmic compartment of a single human erythrocyte ghost (right circle) compared to a cytometer calibration sphere (left circle). Alphanumerics: upper = date (month:day:year), lower = time (min:s:hundredths of s). Buffer in medium and cytoplasmic compartments is 20 mM NaP_i (pH 8.5). Pulse occurs at reference time 00:16:00 (= 16.00 s), exactly. (A) Prepulse image. (B,C) Image with visible cloud (arrows) above hemisphere facing negative electrode. (D,E) Image of residual fluorescence in erythrocyte ghost after cloud has dissipated. Electric field in parallel to plane of micrographs. Electrodes are: plus (+), bottom of frame; negative (−), top of frame.

fluorescence lost per pulse (range 0.10–0.21) in individual membranes may reflect the heterogeneity in pore diameter, number, or lifetime. This fraction was constant for a given membrane as long as the next pulse was the same as the previous pulse and the same membrane was measured.

The observation that the loss of smaller molecules occurred with fewer pulses than when larger molecules were used qualitatively indicated that the electropore radius quickly decreases after opening but in a time-dependent manner.

4. DISCUSSION

The fact that the pulse-induced loss of fluorescence labels occurs in increments (i.e. a large immediate loss over a very short interval is followed by little or no loss over a much longer interval) shows that electropores open to some finite (peak) radius for a finite time and then reseal rapidly.

Losses of fluorescent label from the ghosts after four 0.6 ms pulses were comparable to the losses after one 1.2 ms pulse. This trend is in general agreement with previous studies [1–15]. Since the 0.6 ms pulses do not induce a visible cloud (thus not revealing their location) then the electropores may have a smaller peak radius, be fewer in number, or may reclose at a slower rate. Additional studies will be required to identify the relative contributions of these possibilities.

Since continuous loss of fluorescence occurred after the pulse only when NBD-G was used as a probe, the pores must reclose to a residual radius which is smaller than LY (0.75 nm) but larger than NBD-G (0.45 nm) and then stay at that radius.

Pulses did not induce the leakage of FM, FB, or RP even though these probes are smaller than the largest dextran (156 kDa) used. However, pulses induced leakage of the FM when the ghosts were resealed in the presence of the buffer previously adjusted to pH 6.0, below the isoelectric point (p*I* 7.0) of myoglobin. This suggests that the net charge on the protein may be an important factor. A partial retention of the pulse-induced electric charge build-up on the membrane surrounding the pore may produce an electric field in the vicinity of the electropores which could either permit or prevent the efflux of the protein depending on its net charge (fig.3). Alternatively, an exponentially decaying pulse may surround the membranes with an electric field of sufficient strength after many decay half-times to develop an electrophoretic force to oppose the diffusion force. Lastly, the in-

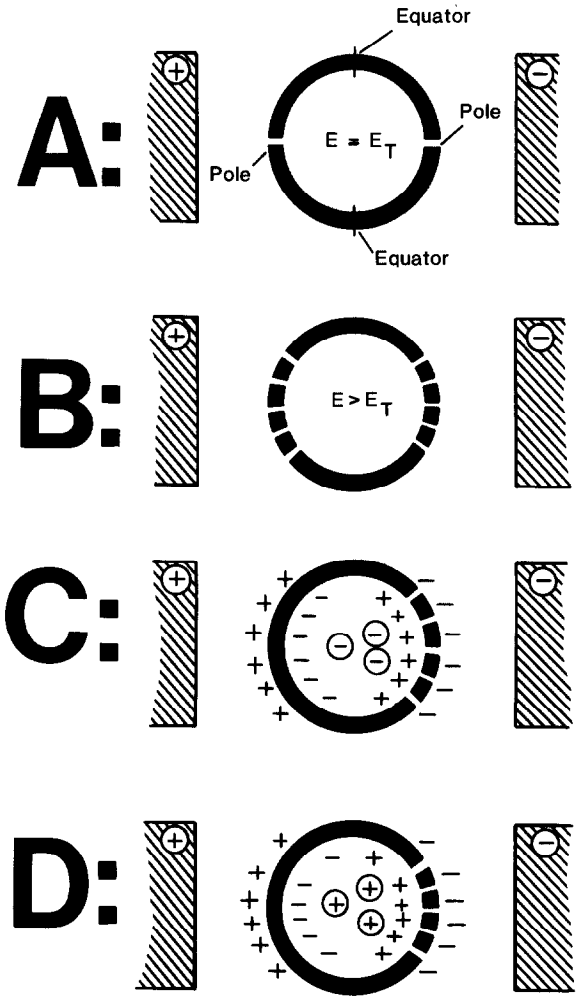

Fig.3. Location of electropores with respect to electric field. (A) One electropore at pole of each hemisphere when induced electric field strength, E, is equal to the minimum transmembrane electric field strength needed to cause dielectric breakdown, E_T. (B) Additional electropores induced at greater distance from poles when $E > E_T$. (C) Net negative charged entity inside spherical membrane is inhibited from diffusing through electropores if movement is against transmembrane electric field. (D) Net positive charged entity inside spherical membrane can diffuse out since movement is in same direction as electric field in vicinity of pore. A,B adapted from fig.1 of [6] and fig.3 of [24]. C,D based on experimental data obtained in this study (see text).

duction of 'flip sites' [23] may lead to a redistribution of fixed charges between the inner and outer leaflets of the bilayer. This new distribution could lead to a local electric field around electropores which could permit or prevent efflux depending on the net charge of the diffusing molecule. LY should also have a net negative charge in our experiments, but in contrast, efflux was observed at pH 8.5. We otherwise have no explanation for this observation. Possibly the role of charge is limited with small molecules such as LY.

Frame by frame playback of video recordings showed that a cloud of fluorescence appeared over only the cathodal hemispheres of ghosts loaded with FD (10 kDa) (fig.1). This indicated that more, larger, or longer-lived pores were induced in that hemisphere. During the lifetime of the cloud, fluorescent molecules from the interior of the labeled ghost membrane were diffusing into the center of this cloud at about the same rate at which they diffused away from the cloud to the background. Because a similar pulse-induced cloud appeared only above the cathodal hemisphere of LY-loaded ghosts the induced pores in the hemisphere facing the positive electrode could (i) never be larger than about 1–2 nm, (ii) be very low in number, or (iii) have a very short lifetime, or some combination of all three. The assumptions used in making the calculations may thus have to be refined. This shows that symmetrical pore formation in both hemispheres of a spherical membrane (fig.3) as previously presented [6,24] does not occur.

In a related study, Mehrle et al. [25] also suggested that pulses induce more, larger, or longer-lived electropores in one hemisphere of individual pulse-treated oat mesophyl protoplasts. Their experiments, which did not measure electropore lifetimes or characterize diameters or numbers, revealed that the pulse-induced permeability increase was preferentially located in the hemisphere oriented towards the positive electrode. The discrepancy in polarity may be due to differences in experimental conditions and properties of the membranes used.

ACKNOWLEDGEMENTS

The expert technical assistance of Ms Veena Kapoor is gratefully acknowledged. We thank L.X. Finegold, R. Korenstein, M. Blank, W.W. Stewart and P. Lelkes for useful discussions.

REFERENCES

[1] Neumann, E. (1984) Bioelectrochem. Bioenerg. 13, 219–223.
[2] Tsong, T.Y. (1983) Biosci. Rep. 3, 487–505.
[3] Knight, D.E. and Scrutton, M.C. (1986) Biochem. J. 234, 497–506.
[4] Pilwat, G., Richter, H.-P. and Zimmermann, U. (1981) FEBS Lett. 133, 169–174.
[5] Zimmermann, U. (1982) Biochim. Biophys. Acta 694, 227–277.
[6] Zimmermann, U., Vienken, J., Halfmann, J. and Emeis, C.C. (1985) in: Advances in Biotechnological Processes (Mizrahi, A. and Van Wezel, A.L. eds) vol.4, pp.79–150, Alan R. Liss, New York.
[7] Dimitrov, D.S. and Jain, R.K. (1984) Biochim. Biophys. Acta 779, 437–468.
[8] Sowers, A. (1986) J. Cell Biol. 102, 1358–1362.
[9] Benz, R. and Zimmermann, U. (1981) Biochim. Biophys. Acta 640, 169–178.
[10] Kinosita, K. and Tsong, T.Y. (1979) Biochim. Biophys. Acta 554, 479–497.
[11] Knight, D.E. and Baker, P.F. (1982) J. Membrane Biol. 68, 107–140.
[12] Neumann, E. and Rosenheck, K. (1972) J. Membrane Biol. 10, 279–290.
[13] Teissie, J. and Tsong, T.Y. (1981) Biochemistry 20, 1548–1554.
[14] Kinosita, K. and Tsong, T.Y. (1977) Biochim. Biophys. Acta 471, 227–242.
[15] Schwister, K. and Deuticke, B. (1985) Biochim. Biophys. Acta 816, 332–348.
[16] Sowers, A. (1984) J. Cell Biol. 99, 1989–1996.
[17] Lieber, M.R. and Steck, T.L. (1982) J. Biol. Chem. 257, 11659.
[18] Granath, K.A. and Kvist, B.E. (1967) J. Chromatogr. 28, 69–81.
[19] Speizer, L., Haugland, R. and Kutchai, H. (1985) Biochim. Biophys. Acta 815, 75–84.
[20] Stewart, W.W. (1981) Nature 292, 17–21.
[21] Henderson, R. and Unwin, P.N.T. (1975) Nature 257, 28–32.
[22] Nowotny, A. (1969) in: Basic Exercises in Immunochemistry, pp.17–19, Springer, New York.
[23] Dressler, V., Schwister, K., Haest, C.W.M. and Deuticke, B. (1983) Biochim. Biophys. Acta 732, 304–307.
[24] Zimmermann, U. (1983) Trends Biotechnol. 1, 149–155.
[25] Mehrle, W., Zimmermann, U. and Hampp, R. (1985) FEBS Lett. 185, 89–94.